Tool wear and surface quality in milling of a gamma-TiAl intermetallic

Tool wear and surface quality in milling of a gamma-TiAl intermetallic

Paolo Claudio Priarone · Stefania Rizzuti · Giovanna Rotella · Luca Settineri

Abstract Advanced structural materials for high-temperature applications are often required in aerospace and automotive fields. Gamma titanium aluminides, intermetallic alloys that contain less than 60 wt.% of Ti, around 30–35 wt.% of aluminum, and other alloy elements, can be used as an alternative to more traditional materials for thermally and mechanically stressed components in aerospace and automotive engines, since they show an attractive combination of favorable strength-to-weight ratio, refractoriness, oxidation resistance, high elastic modulus, and strength retention at elevated temperatures, together with good creep resistance properties. Unfortunately such properties, along with high hardness and brittleness at room temperature, surface damage, and short and unpredictable tool life, undermine their machinability, so that gamma-TiAl are regarded as difficult to cut materials. A deeper knowledge of their machinability is therefore still required. In this context the paper presents the results of an experimental campaign aimed at investigating the machinability of a gamma titanium aluminide, of aeronautic interest, fabricated via electron beam melting and then thermally treated. Milling experiments have been conducted with varying cutting speed, feed, and lubrication conditions (dry, wet, and minimum quantity lubrication). The results are presented in terms of correlation between cutting parameters and lubrication condition with tool wear, surface hardness and roughness, and chip morphology. Tool life, surface roughness, and chirp morphology showed dependence on the cutting parameters. Lubrication conditions were observed to heavily affect tool wear, and minimum quantity lubrication was shown to be by far the method that allows to extend tool life.

Keywords Intermetallic alloy · Machinability · Tool wear · Lubrication

P. C. Priarone · S. Rizzuti (✉) · G. Rotella · L. Settineri
Department of Production Systems and Business Economics,
Politecnico di Torino,
Corso Duca degli Abruzzi,
10129 Turin, Italy
e-mail: stefania.rizzuti@polito.it

1 Introduction

Gamma titanium aluminides (γ-TiAl) are intermetallic alloys that contain 44–48 atomic percent Al (32–35 in weight percent), with element additions of Cr, or Mn to increase ductility, and Nb to improve strength and oxidation resistance; γ-TiAl alloys can be used as an alternative to Ni-based superalloys for thermally and mechanically stressed components in aerospace and automotive engines [1, 2]. Gamma-TiAl alloys show approximately half the density of Ni superalloys, high strength/weight ratio, high stiffness, high refractoriness, and high temperature strength. Furthermore, they show fatigue resistance values close to 100% of yield strength [2].

In spite of these advantages, γ-TiAl alloys show some drawbacks: low ductility at room temperature, which typically ranges between 0.3% and 4% in terms of elongation at rupture (depending on composition and microstructure), together with low fracture toughness. Furthermore, these characteristics, along with low thermal conductivity and chemical reactivity with many tool materials, make γ-TiAl difficult to cut materials. Other features impairing machinability are the sensitivity to strain rate, with a strong tendency to hardening, the saw tooth chip shape, the built-up edge and the presence of abrasives in the alloy microstructure that contribute to accelerated wear of the cutting edge, and the formation of large crater

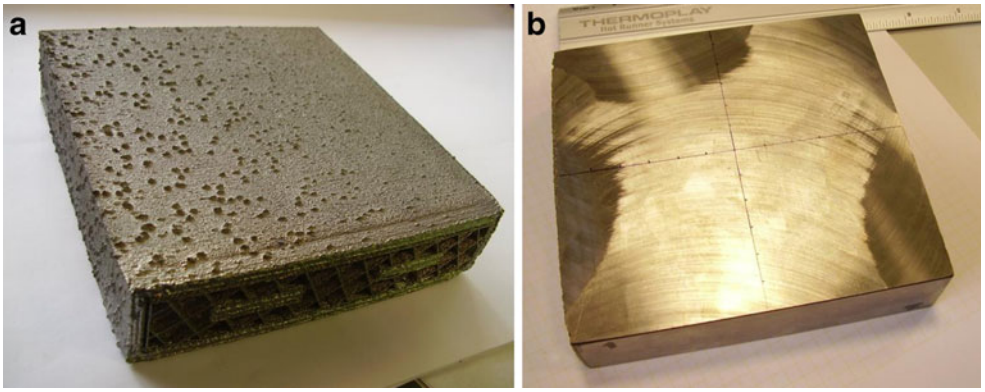

Fig. 1 Sample used for the milling tests: as provided by the supplier (**a**) and after preparation for the milling tests (**b**)

wear on the rake face and evident chipping phenomena. On the workpiece side, we can observe that these unfavorable characteristics translate into surface hardening, residual stresses, poor finish, and presence of microcracks, impairing fatigue strength of the finished component [3–5]. Nevertheless, the interest for gamma titanium aluminides applications is high because of highly stressed components in the automotive and aerospace sectors, such as engine valves for high-performance engines, exhaust nozzles, and turbine blades, and there still is a need for further studies, particularly to fully understand the machinability of these alloys with conventional or nonconventional processes and to optimize process parameters.

In this paper the results of an experimental campaign aimed at investigating the machinability of a γ-TiAl alloy produced via electron beam melting (hereafter EBM) are reported. Milling experiments have been conducted with varying cutting speed, feed, and lubrication conditions. Machining results are presented and discussed in terms of tool wear, surface hardness and roughness, surface integrity, and chip morphology.

2 Experimental setup

The milling tests were carried out on a γ-TiAl specimen with rectangular shape (120×120×30 mm), obtained via EBM and subsequently thermally treated. The sample is illustrated in Fig. 1. EBM is an additive manufacturing process for metal parts that starts from powders and melts them layer after layer with an electron beam in a high vacuum. Unlike some metal-sintering techniques, the parts are almost fully dense and void free. The high vacuum makes it suited to manufacture parts in reactive materials with high affinity for oxygen, e.g., titanium [6, 7]. The process is followed by a heat treatment to improve density and release residual stresses. The applied heat treatment was 5 h at 1,095°C, then hot isostatic pressing for 4 h at 1,285°C, then 2 h at 1,305°C.

The chemical composition of the alloy is listed in Table 1, while the main properties at room temperature are reported in Table 2. Furthermore, the specimen showed an average initial hardness of 273 HV_{30} (with a standard deviation of 5.2 HV_{30}).

Specimens to perform microstructural analysis were randomly cut from the workpiece; the samples were ground and polished with suspension of colloidal silica (SPM) up to 0.1 μm abrasive particle size, then etched in a Keller solution of 100 ml H_20, 2.5 ml HNO_3, 1.5 ml HCl, and 1 ml HF prior to inspection. A microstructural observation on the material reveals a typical lamellar structure, as shown in Fig. 2, with a different orientation of lamellae. The microstructure is not always homogeneous, as shown in the Fig. 3, where some porosity can be observed. As expected, the EBM fabrication process does not deliver a material with full density [8, 9]: in the present case, density is around 98%.

The experimental tests were performed using a three-axis Cortini M500/F1 vertical CNC milling machine. The machine has a continuously variable spindle that reaches up to 8,000 rpm, with a peak power of 3.7 kW and a maximum torque of 24 Nm.

Tools used in the experiments were 10-mm diameter Vergnano F405 carbide ISO K30/K40 end mills, with four

Table 1 Chemical composition of the machined γ-TiAl alloy (in weight percent)

Al	Nb	Cr	O	N	C	Fe	H	Others	Ti
32.0–33.5	4.5–5.1	2.2–2.6	<0.08	<0.02	<0.015	<0.04	<0.001	<0.05	Balance (<60%)

Table 2 Mechanical properties of γ-TiAl alloy

Tensile strength	345 MPa
Yield strength (0.2% offset)	276 MPa
Elongation, percent in 4D	0.5

uncoated edges. Table 3 reports the geometrical parameters of the tools, while a new cutting tool is shown in Fig. 4.

In order to investigate the alloy's machinability, the experimental plan listed in Table 4 was carried out. Axial depth of cut d_a and radial depth of cut d_r were kept constant and both equal to 0.3 mm, while cutting speed V and feed per tooth f were assumed as independent input variables. The cutting parameters were changed according to a 2^2+* experimental plan, enriched by other experimental points explored to better point out the dependence on the lubrication conditions [10]. The milling operations were undertaken in down-milling direction, in dry, MQL, and wet conditions. MQL lubrication was performed with a Novatea Accu-Lube Minibooster microlubrication system, with a vegetal lubricant flow of 0.3 ml/min at an air pressure of 5.5 bars, while wet cutting was carried out with a 5% emulsion of mineral oil in water, with a flow of 10 l/min. Three repetitions for each experimental point have been performed, and the tests were executed following a random order to reduce the time-dependence effects.

Tools were periodically examined in order to measure wear at different cutting times, by means of a stereo microscope Leica MS5 (with ×40 magnification), equipped with a high-resolution camera Leica DFC280 for image acquisition. The tests were performed until the fixed limit of 100 μm for tool wear was reached: the parameter used to evaluate tool wear as a function of processing time is the maximum value between flank wear and corner wear measured on the secondary flank surface, as shown in Fig. 5. Such restrictive condition, typical of a finishing operation, has been chosen since the manufacturing of a γ-TiAl component typically starts from a semimanufactured

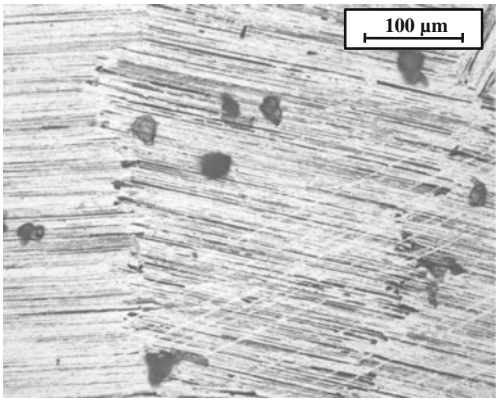

Fig. 3 Optical micrograph showing porosity

part, obtained by Rapid Manufacturing processes or casting processes, in a shape that is close to the finished part. Therefore cutting is often limited to semifinishing or finishing. Furthermore, surface integrity and tolerances of a component made of γ-TiAl alloy are critical requirements that must meet the severe specifications of the automotive and especially aerospace industry. In fact excessively worn tools generate more deformations, with surface hardening, residual stresses, and poor finish.

The roughness of the milled surface was measured by a Hommelwerke Tester T1000 according to DIN EN ISO 4287. In particular, the arithmetic mean roughness value R_a, the maximum roughness profile height R_t, the skewness R_{sk} and the curtosis roughness R_{ku} were measured in the feed direction. It is useful to remark that R_{sk} and R_{ku} are important indexes when the machined surface load-bearing capability needs to be investigated.

The HV_{30} hardness of the generated surface was measured by an Emcotest M4U 025 universal hardness tester, according to the reference standard DIN EN ISO 6507. Microstructural analysis of the material and observation of the generated surface has been performed using an inverted optical microscope Leica MEF4U with magnification up to ×1,880, while chip morphology was investigated

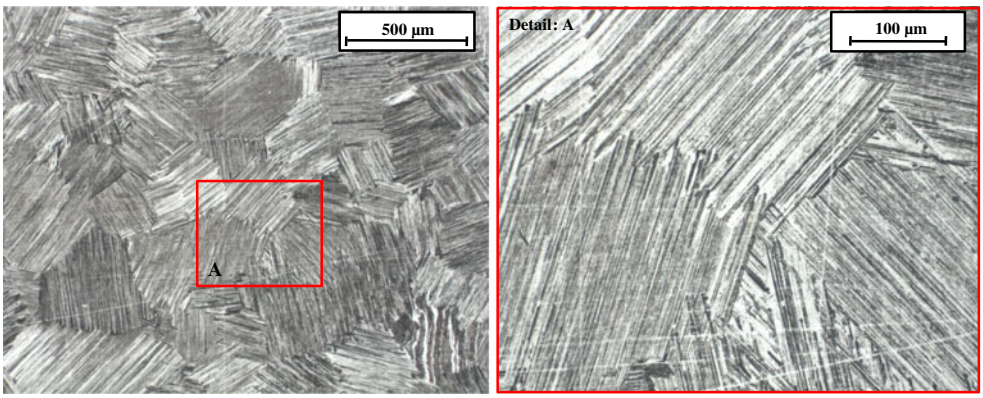

Fig. 2 Lamellar microstructure of the sample

Table 3 End mills geometrical parameters

Parameter	Value
Mill diameter (mm)	10
Length of cut (mm)	23
Cutting tool angle (°)	12
Helix angle (°)	30
Axial primary relief angle (°)	6
Axial secondary clearance angle (°)	16
End cutting edge concavity angle (°)	2
Radial rake angle (°)	12

by a scanning electron microscope LEO 1450 VP, with theoretical resolution equal to 10 nm.

Table 4 Experimental plan

	Test	Lubrication condition	V (m/min)	f (mm/tooth)
2^2+*	1	DRY	35	0.06
	2		35	0.10
	3		50	0.08
	4		71	0.06
	5		71	0.10
	6	DRY	50	0.10
	7	WET	50	0.08
	8	MQL	35	0.10
	9		50	0.08
	10		50	0.10
	11		71	0.10

3 Results and discussion

The obtained experimental data on tool wear, surface roughness, and hardness have been analyzed: Table 5 summarizes the results discussed below.

3.1 Tool wear

Figure 6 illustrates examples of worn tools, for the cases V= 50 m/min and f=0.08 mm/tooth, after 30 min of cutting time and for each lubrication condition. From the observation of the worn tools, it can be assessed that the tool fails more often for corner wear, especially in the case of higher feed per tooth. This is caused by chipping of the cutting edge tip.

Figure 7 shows two SEM-backscattered images of the tool rake face and of the tool tip. The backscattered images show some adhesion of workpiece material, besides evident wear signs and microcracks.

The results in terms of tool life listed in Table 5 highlight that tool wear rate, in dry condition, increases as the feed per tooth and the cutting speed increase, as expected. These trends resulted also in agreement with the results reported by Branoagirre for other gamma-TiAl alloys, manufactured as solidified ingot and extruded after solidification [11, 12]. In dry milling, the experimental data for tool life estimation are well fitted by the following full quadratic model (correlation index R=0.99), whose behavior is shown in Fig. 8:

$$T_L = 658.38 - 6.1748 \cdot V - 9517.6 \cdot f + 41.555 \cdot V \cdot f + 0.014238 \cdot V^2 + 36593 \cdot f^2$$

In addition, variability of tool wear results for the repeated tests remained lower than 10% in terms of relative range.

Lubrication condition is also a factor strongly affecting wear mode and tool life. Typical tool wear curves are

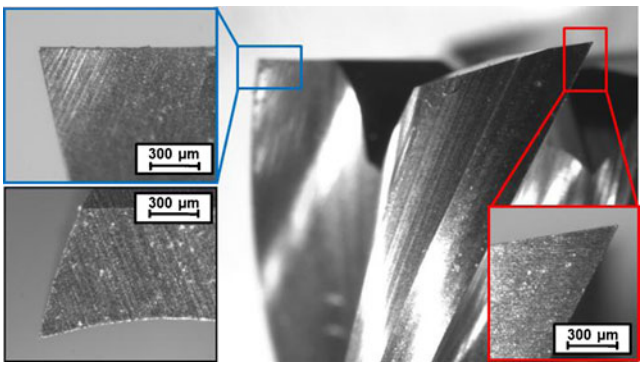

Fig. 4 Uncoated Vergnano F405 carbide end mill

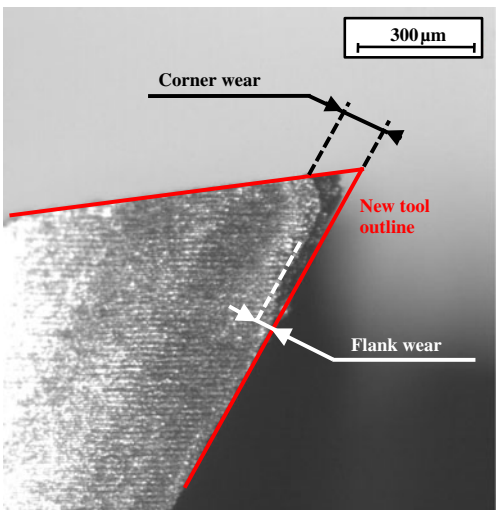

Fig. 5 Tool wear measurement criteria

Table 5 Experimental results

Lubrication condition	V (m/min)	f (mm/tooth)	Tool life (min)	Surface hardness (HV_{30})	Roughness indexes			
					R_a (μm)	R_t (μm)	R_{sk}	R_{ku}
Dry	35	0.06	107.6	297	0.22	1.73	−0.03	3.17
Dry	35	0.10	19.3	300	0.31	2.62	−0.05	3.28
Dry	50	0.08	24.2	299	0.22	1.81	−0.12	3.31
Dry	71	0.06	29.4	298	0.19	1.54	−0.07	3.25
Dry	71	0.10	0.95	310	0.22	1.66	−0.05	2.98
Dry	50	0.10	7.2	316	0.24	2.03	−0.09	3.25
Wet	50	0.08	5.8	299	0.26	2.38	−0.36	3.44
MQL	35	0.10	133.3	299	0.28	2.46	−0.20	3.35
MQL	50	0.08	145.1	301	0.28	2.52	−0.28	3.45
MQL	50	0.10	49.0	310	0.27	2.46	−0.19	3.38
MQL	71	0.10	7.1	294	0.32	3.03	−0.26	3.53

shown in Fig. 9, for the case f=0.10 mm/tooth, and in Fig. 10 for the three different lubrication conditions (wet, dry, and MQL). Each experimental point plotted into the graphs is the average value of the wear measured on the four edges of the mill.

In the case of wet cutting, the cutting edge abrupt cooling causes severe thermal shocks, leading to the breakage of the cutting edges. This explains the very low tool life achieved. MQL appears to be, by far, the most advantageous lubricating system in terms of tool wear.

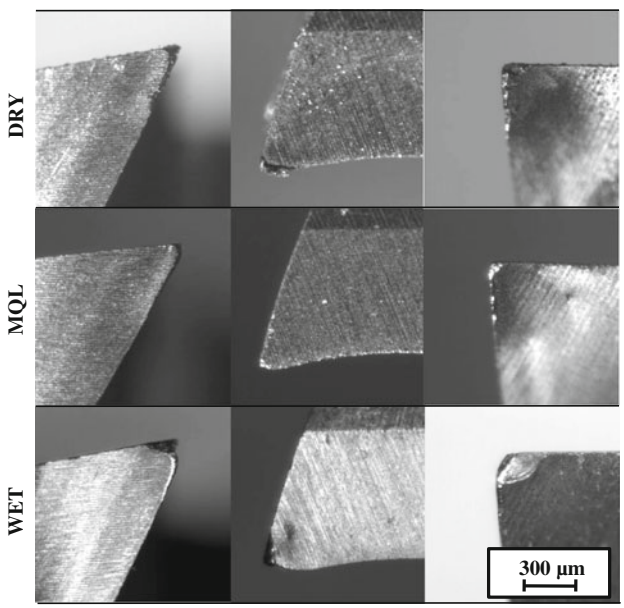

Fig. 6 Worn tools for the case of V=50 m/min and f=0.08 mm/tooth, after 30 min of cutting time

3.2 Surface hardness

Figures 11 and 12 show the trends of the surface hardness as a function of processing time. Each point in the graph is the average value of five experimental measurements. In addiction Table 5 reports the estimated hardness corresponding to the maximum tool life. The effects of cutting time are visible: hardness increases as a result of strain hardening due to tool wear. This occurrence is common to all tests performed.

In dry conditions, as far as the effects of the cutting parameters are concerned, it can be assessed that the surface hardness increases as the feed per tooth increase, and this trend is stronger in the range between 0.08 and 0.1 mm/tooth. On the other hand, the dependence on the cutting speed is more complex: this is due to a prevailing hardening effect at intermediate speed, compensated by the temperature increasing at higher speed that softens the surface [13].

The effects of the different lubrication conditions on hardness are more complex to explain: in wet conditions, the lubrorefrigerant has a hardening effect, as if the upper material layers underwent a heat treatment. In dry conditions, this effect is not present, but the high friction coefficient and therefore the high strain keep the hardness relatively high. In MQL conditions, the low friction coefficient, combined with the gentle cooling effect, limits strain hardening with respect to the other cutting conditions [13].

3.3 Surface roughness

Table 5 shows the results of the roughness measurements: the values are the average of all measurements taken until

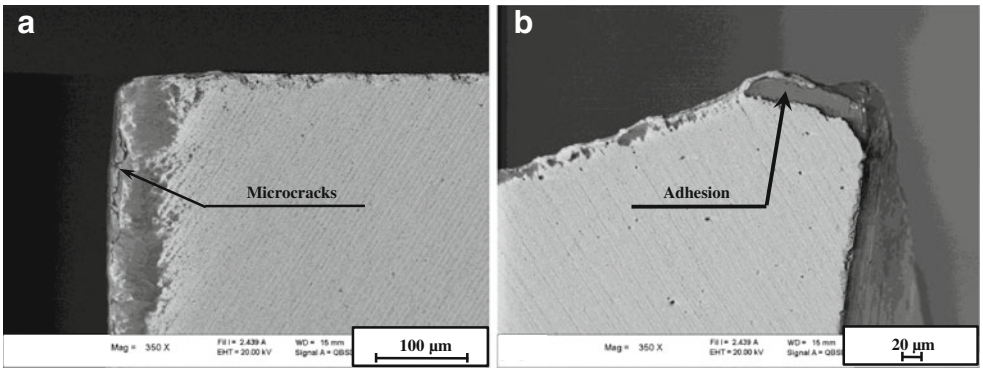

Fig. 7 Backscattered SEM images of one cutter after machining. Tool rake face (**a**) and tool tip (**b**), for the case of V=50 m/min and f=0.08 mm/tooth, dry conditions after 30 min of cutting time, respectively, show microcracks and material adhesion signs

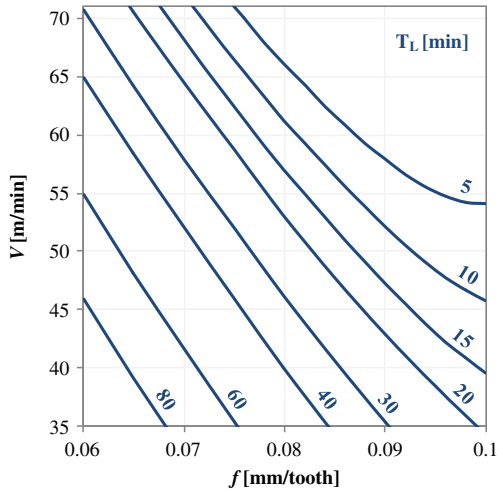

Fig. 8 Tool life T_L (in minutes) as a function of V and f, for dry lubrication condition. The model used is reported in the full quadratic model as shown in Section 3.1

the tool wear limit was reached. As for the generated surface quality, the mean roughness R_a and the maximum roughness profile height R_t present a clear trend vs. the cutting speed and the feed per tooth. As expected, in dry lubrication conditions, R_a and R_t indexes decrease as the cutting speed increases and the feed per tooth decreases.

In Fig. 13 a full quadratic model of R_t as a function of cutting speed and feed per tooth in dry conditions is represented, according to the following equation (correlation index R=0.99):

$$R_t = 0.11522 - 0.03584 \cdot V + 62.784 \cdot f - 0.52924 \cdot V \cdot f + 0.000587 \cdot V^2 - 139 \cdot f^2$$

R_a has a very similar behavior.

On the other hand, Table 5 shows that R_{ku} and R_{sk} have a more complex dependence on the cutting speed and feed

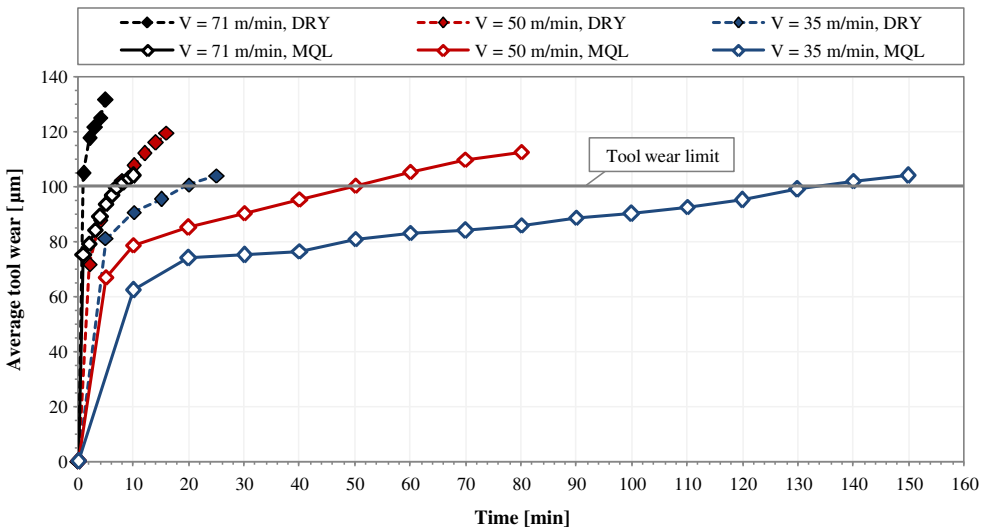

Fig. 9 Typical tool wear curves for the case f=0.10 mm/tooth

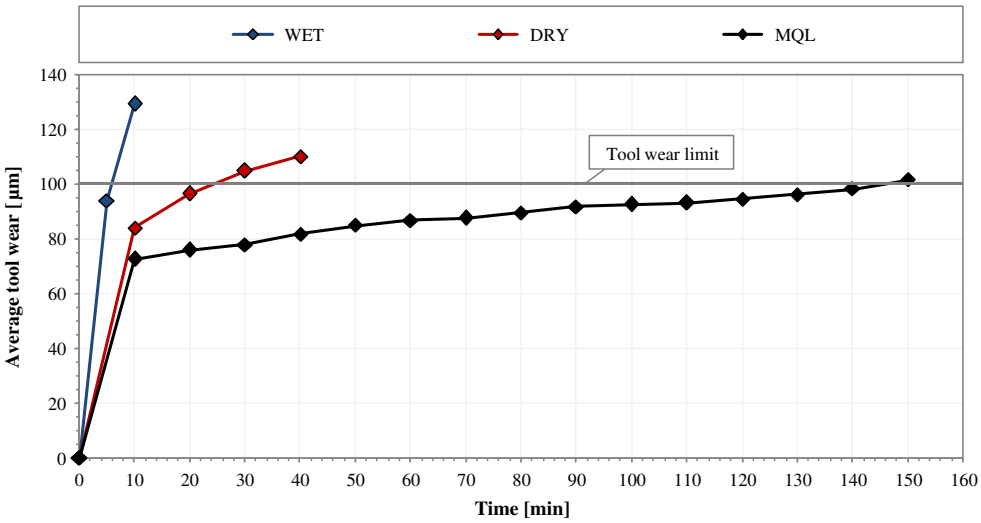

Fig. 10 Typical tool wear curves for the case V=50 m/min, f=0.08 mm/tooth

per tooth: R_{ku} shows a maximum for the intermediate cutting speed and feed and decreases thereafter, while R_{sk} behaves in the opposite way. This effect is due to the characteristics of the chip formation mechanism that, for intermediate values of cutting speed and feed, generates microcraters on the machined surface, being the material obtained via a powder-melting process [8, 9].

The effects of different lubrication systems on the surface roughness do not follow strictly the indications of the literature, being the results for dry cutting better than in the other cases ([5] and ref. therein). In Fig. 14 the generated surface is observed, in the case of V=50 m/min and f=0.08 mm/tooth, in dry and MQL conditions. The presence of microcraters is evident, due to the microstructure of the sample, manufactured via a powder-compacting process [8, 9] and to the chip formation mechanism. This phenomenon is less evident at different cutting speeds.

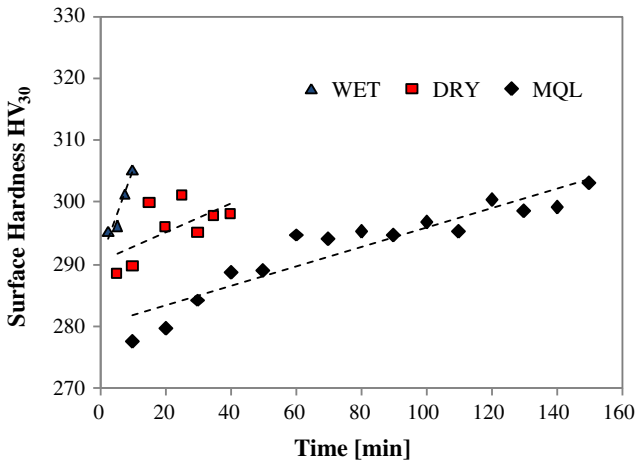

Fig. 12 Hardness of the generated surface for the case V=50 m/min and f=0.08 mm/tooth, for different lubrication conditions

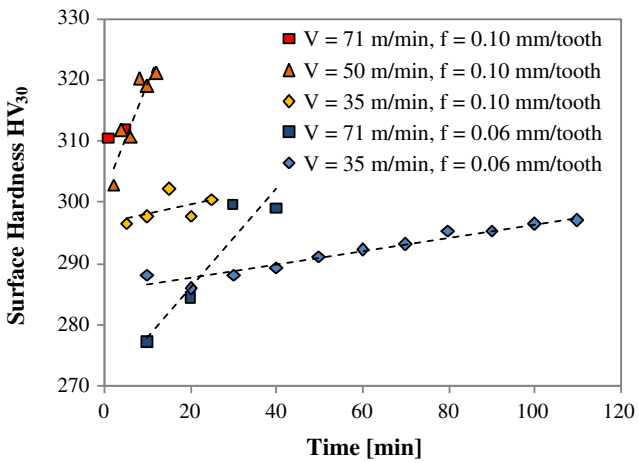

Fig. 11 Hardness of the generated surface for dry lubrication conditions

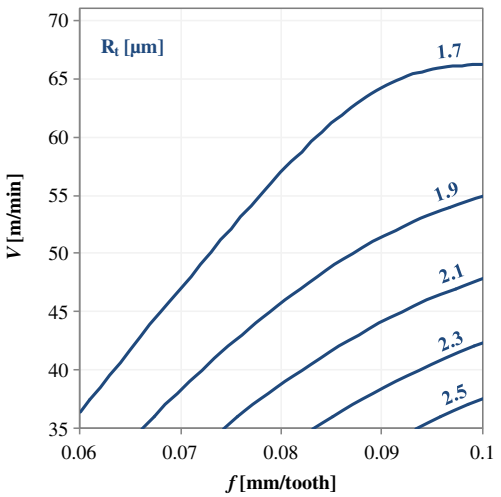

Fig. 13 Computed model of R_t (in micrometers) vs. V and f for dry lubrication condition

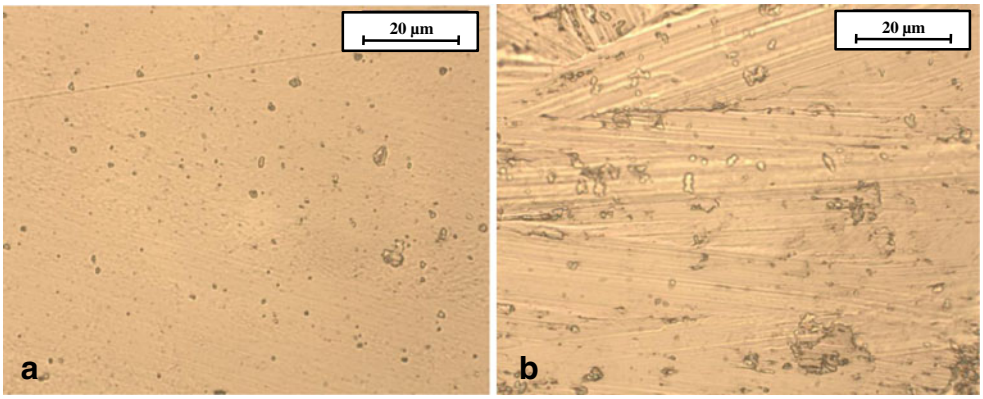

Fig. 14 Micrograph of the generated surface (×1,000), V=50 m/min, f=0.08 mm/tooth, for the dry (**a**) and MQL (**b**) conditions

3.4 Chip morphology

Figures 15 and 16 obtained by SEM show, with different magnifications, the chip morphology for f=0.06 mm/tooth and for dry lubrication condition, at different cutting speeds. Chips are in general very small, almost powder like, and with sharp edges, due to the low deformability of the material.

Looking at Fig. 15, a clearly perceivable increase in the average chip size at higher cutting speed can be observed: this phenomenon is due to a prevailing effect of the temperature increase (resulting in a greater deformability of the material) rather than of the higher strain rate. A further effect of the higher temperature is that the chip width is higher and more regular. The higher chip temperature is confirmed by the different color of the chip that is darker at higher cutting speed, an effect that cannot be seen from the SEM images.

From the observation of Fig. 16, obtained with higher magnification, we can clearly see the shear planes and the lower thickness of the lamellae as the cutting speed increases. The chip formation mechanism recalls the "card deck" model of Piispanen [14].

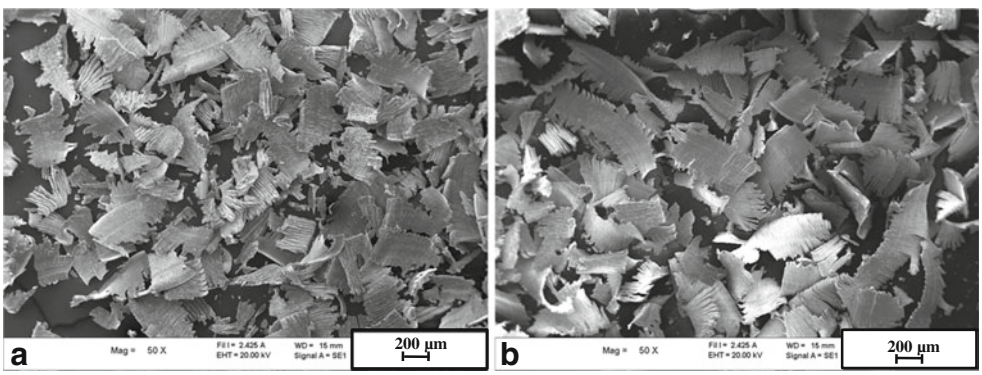

Fig. 15 Chip morphology (×50) for f=0.06 mm/tooth, V=35 m/min (**a**) V=71 m/min (**b**)

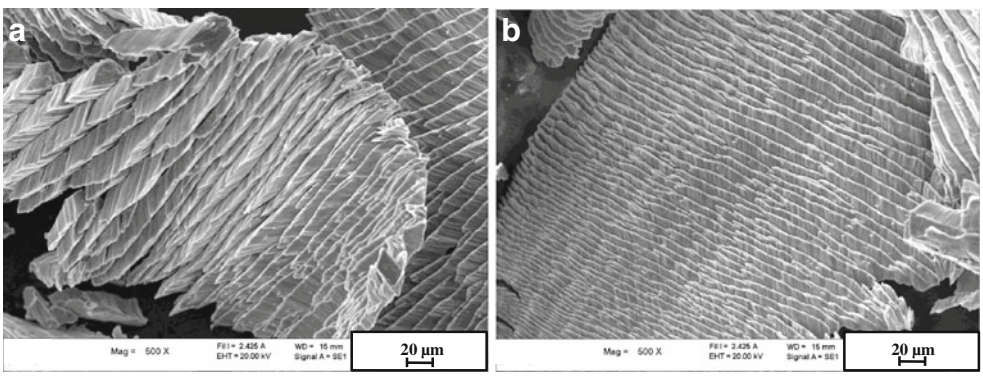

Fig. 16 Chip morphology (×500) for f=0.06 mm/tooth, V=35 m/min (**a**) V=71 m/min (**b**)

4 Conclusion

In this paper, the results of milling experiments conducted on a particular γ-TiAl, manufactured starting from powders via electron beam melting, followed by a particular thermal treatment are presented. The experiments are conducted in finishing or semifinishing cutting conditions, with three different lubrication conditions.

The results show that, in dry conditions, tool life is well modeled by a full quadratic equation as a function of cutting speed and feed per tooth. Lubrication conditions heavily affect tool wear: in wet conditions, the tool wear rate is higher than in dry conditions, while minimum quantity lubrication is by far the method that allows to extend tool life.

Surface roughness parameters show dependence on the cutting parameters, at least in the explored range. R_a and R_t increase with the tool wear and show classical dependence on cutting speed and feed, while the nonmonotonic behavior of R_{sk} and R_{ku} on cutting speed and feed is due to the mechanism of chip formation that generates microcraters on the surface with intermediate values of speed and feed.

Chip morphology shows a typical "card deck" chip formation mechanism, with chip length and width dependent on the cutting speed. Further work is needed to optimize tool geometry in terms of cutting angles and cutting edge pretreatment as well as to explore the effects of advanced tool coatings.

Acknowledgments The authors wish to acknowledge the contribution of the Region Piedmont and of the EU that funds this research activity in the framework of a MANUNET Project, the company Fratelli Vergnano S.r.l. and in particular Mr. Guido Vergnano for supplying the tools, and the company AVIOPROP for supplying the workpiece material.

References

1. Austin CM (1999) Current status of gamma titanium aluminides for aerospace applications. Curr Opin Solid State Mater Sci 4:239–242
2. Loria EA (2000) Gamma titanium aluminides as a prospective structural materials. Intermetallics 8:1339–1345
3. Aspinwall DK, Dewes RC, Mantle AR (2005) The machining of γ-TiAl intermetallic alloys. Annals of the CIRP 54(1):99–104
4. Mantle AR, Aspinwall DK (2001) Surface integrity of a high speed milled gamma titanium aluminide. J Mater Process Technol 118:143–150
5. Sharman ARC, Aspinwall DK, Dewes RC, Bowen P (2001) Workpiece surface integrity considerations when finish turning gamma titanium aluminide. Wear 249:473–481
6. Cormier D, Harrysson O, Mahale T, West H (2007) Freeform fabrication of titanium aluminide via electron beam melting using prealloyed and blended powders. Research Letters in Materials Science, Hindawi Publishing Corporation 1–4
7. Yu KO (2001) Modeling for casting and solidification processing. Taylor & Francis, New York
8. Petropoulos GP, Pandazaras CN, Davim JC, West H (2010) Surface texture characterization and evaluation related to machining. Springer-Verlag, London
9. Cotterell M, Byrne G (2008) Dynamics of chip formation during orthogonal cutting of titanium alloy Ti–6Al–4V. Annals CIRP 57 (1):93–96
10. Montgomery DC, Runger GC (2007) Applied statistics and probability for engineers. Wiley, London
11. Beranoagirre A, Lopez de Lacalle LN (2010) Optimizing the milling of titanium aluminide alloys. Int J Mechatron Manuf Syst 3–5(6):425–436
12. Beranoagirre A, Lopez de Lacalle LN (2009) Milling of gamma TiAl intermetallic alloys. AIP Conf Proc. doi:10.1063/1.3273661
13. Shaw MC (2005) Metal cutting principles. Oxford University Press, New York
14. Piispanen V (1937) Lastunmuodostumisen Teoriaa (Theory of chip formation). Teknillinen Aikakauslenti 27:315–322